(min,+) Algebra and Analysis, a powerful tool for non-linear Mathematics

Dr A. KENOUFI

European Interdisciplinary Academy of Sciences (EIAS), Paris, France
Scientific COnsulting for Research & Engineering (SCORE), Strasbourg, France

Moscow, April 25^{th}, 2019

- Dr Michel GONDRAN, University of Paris-Dauphine, France.
  European Interdisciplinary Academy of Sciences (EIAS), Paris, France.
  michel.gondran@polytechnique.org
- Dr Alexandre GONDRAN, Ecole Nationale de l'Aviation Civile (ENAC), Toulouse, France.
  alexandre.gondran@enac.fr
- Dr Thierry LEHNER
  Observatory of Paris-Meudon (LUTH), Meudon, France.
  thierry.lehner@obspm.fr

1. Tropical and idempotent algebra
   - Dioids, semi-rings, and semi-fields
   - Deformation of dioids
2. Elements of idempotent analysis
   - Integration
   - Scalar product
3. Non-linear problems analysis with $(\min, +)$
   - The shortest path problem in graph theory and Bellman's Optimality Theorem
4. Fractals & Multi-fractals
   - Self-similar sets and Hausdorff dimension
     - Hölder exponents and multi-fractal spectrum
     - Heuristic approach of multi-fractal analysis
     - Thermodynamic formalism
   - Wavelet-transform modulus-maxima method (WTMM)
   - Calculations of multi-fractal spectrum

- Comparison between $(\min, +)$-wavelets and WTMM methods
  - Riemann serie
  - Mandelbrot binomial measure

5 Other applications

Tropical and idempotent mathematics find their roots in theoretical informatics and computer sciences, especially in operations research, automation, ...
The term *tropical* has been introduced in honor of the Brazilian mathematician Imre Simon (1943-2009). The main idea driving those new and original mathematics is to develop algebra and analysis on structure which are not fields or rings, but on dioids or semi-rings, eventually semi-fields.

- The first examples of such structures were developed within the so-called idempotent mathematics such (min,+)-algebra and (max,+)-algebra . This is achieved by replacing usual operations such as $+$ and $\times$ with min or max.
- Twenty years before the introduction of $(\min, +)$-analysis by V. P. Maslov *et al* in 1987 and 1992 under the name idempotent analysis, some mathematicians and computer scientists have first defined and used $(\min, +)$-analysis and $(\max, +)$-analysis to solve problems in operation research. Those approaches can be applied to the resolution of many path-finding problems in graphs.

The term *dioid* takes its origin in the work of M. Gondran and was in the book of J. Kutzman about Network Theory, in which he described an algebraic structure made from two monoids. Those unconventional structures are actually and often called tropical or exotic algebra. Semi-rings, semi-fields and dioids are usually named exotic or tropical objects and come up in many applications such as optimal control, graph theory, classical, quantum and statistical physics for example. They are the basic object of the so-called idempotent mathematics.

If one considers a set $X \neq \emptyset$ endowed with two operations : $\oplus$ and $\otimes$ verifying the following conditions :

- $\oplus$ and $\otimes$ are associative, $\oplus$ is commutative, and $\otimes$ is distributive with respect to $\oplus$;
- $\exists\ e_\otimes \in X$ such that $e_\otimes \otimes x = x \otimes e_\otimes = x$ for all $x \in X$;
- $\exists\ e_\oplus \in X$ such that $e_\oplus \neq e_\otimes$ and $e_\oplus \oplus x = x$, and $e_\oplus \otimes x = x \otimes e_\oplus = e_\oplus$ for all $x \in X$;

then $(X, \oplus, \otimes)$ is called a **semi-ring**.

- If $x \oplus x = x$ for all $x \in X$, the semi-ring will be qualified as **idempotent semi-ring**. Moreover, for a semi-ring $(X, \oplus, \otimes)$, if all elements $x \neq e_{\oplus} \in X$ are invertible for $\otimes$, it is called a **semi-field**.
- The binary relation $\textcircled{\leq}$ defined on monoïd $(X, \oplus)$ by $x \textcircled{\leq} y \Leftrightarrow \exists z \in X, y = x \oplus z$ is a pre-order relation (reflexive and transitive) called canonical or standard pre-order. If $\textcircled{\leq}$ is an order (anti-symmetric), $(X, \oplus)$ is then called (canonically) ordered monoïd.
- A semi-ring $(X, \oplus, \otimes)$ such that $(X, \oplus)$ is a (canonically) ordered monoïd is called a **dioid**.
- If $\oplus$ is commutative and idempotent, then the pre-order relation $\textcircled{\leq}$ relation is a canonical order.

- The set of natural numbers $(\mathbb{N}, +, \times)$ with neutral elements 0 and 1, and with $\leq$ as canonical ordered relation, is a dioid, neither a field or a ring.
- Both dioids $\mathbb{R}_{\max,+} = (\mathbb{R} \cup \{-\infty\}, \max, +)$ with neutral elements $-\infty$ and 0, $\mathbb{R}_{\min,+} = (\mathbb{R} \cup \{+\infty\}, \min, +)$ with neutral elements $+\infty$ and 0, and endowed respectively with order relation $\circledleq \equiv \leq$ and $\circledleq \equiv \geq$ are idempotent.

Let $\mathbb{R}^+$ be the semi-ring of all non-negative real numbers (with respect to the usual addition and multiplication).
There are many examples of ordered monoïds, which can be built with mean of algebraic deformation and isomorphism using a parameter $h \in \mathbb{R}^{+*}$ from the monoïds $(\mathbb{R}^+, +)$ and $(\mathbb{R}^+, \times)$.
For any monoïd $(X, \oplus_h) \subset \mathbb{R}$ and any bijection $\Phi_h : X \longrightarrow \mathbb{R}^+$, one can create an isomorphism between X and $\mathbb{R}^+$ by transferring the $\oplus_h$ operation through Φ_h

$$\Phi_h(a \oplus_h b) = \Phi_h(a) + \Phi_h(b), \ \forall a, b \in X,$$

which leads to

$$a \oplus_h b = \Phi_h^{-1}\big(\Phi_h(a) + \Phi_h(b)\big). \tag{1}$$

The same procedure can be done for the $\otimes$ operation as well with

$$a \otimes_h b = \Phi_h^{-1}\big(\Phi_h(a) \times \Phi_h(b)\big). \tag{2}$$

This endows $(X, \oplus_h, \otimes_h)$ with a dioid structure, and particularly $e_\oplus = \Phi_h^{-1}(0)$ and $e_\otimes = \Phi_h^{-1}(1)$.

The deformation parameter h plays the role of the Planck constant in physics, and its limit to zero, can be considered as the semi-classical limit. The following example below is therefore very important for physics applications.

Let's consider the following isomorphism

$$\begin{aligned} \Phi_h \colon (\mathbb{R}, \oplus_h, \otimes_h) &\longrightarrow (\mathbb{R}^+, +, \times) \\ x &\longmapsto e^{-\frac{x}{h}}. \end{aligned} \tag{3}$$

Using equations (1), (2) and (3), one gets $\Phi^{-1} : x \longmapsto -h\ln(x)$, then for all $a, b \in \mathbb{R}^+$,

$$\begin{cases} a \oplus_h b = -h\ln(e^{\frac{-a}{h}} + e^{\frac{-b}{h}}),\ a \otimes_h b = a + b, \\ \lim\limits_{h\to 0^+} \Phi_h^{-1}(0) = +\infty,\ \lim\limits_{h\to 0^+} \Phi_h^{-1}(1) = 0. \end{cases} \tag{4}$$

Since $\otimes_h$ is h-independent, the deformation of the dioid $(X, \oplus_h, \otimes_h)$ for $h \to 0^+$ leads to

$$\lim_{h\to 0^+}(a \oplus_h b) = \min(a, b),\ \lim_{h\to 0^+}(a \otimes_h b) = a + b.$$

This shows that the structure $(\mathbb{R}, \oplus_h, \otimes_h)$ is deformed into $\mathbb{R}_{\min,+} = (\mathbb{R} \cup \{+\infty\}, \min, +)$ when $h \to 0^+$.

Let's consider the one-dimensional heat diffusion equation

$$\frac{\partial u(x,t)}{\partial t} = \frac{h}{2}\frac{\partial^2 u(x,t)}{\partial x^2}, \tag{5}$$

with $h > 0$ a parameter. It is a linear equation since if u_1 and u_2 are both solutions of heat equation, then any linear combination $u = \lambda_1 u_1 + \lambda_2 u_2,\ (\lambda_1, \lambda_2) \in \mathbb{R}^2$, is still a solution.

If one makes the following changes $u(x,t) = \Phi_h(w(x,t))$, and $u_i(x,t) = \Phi_h(w_i(x,t))$, $i = 1, 2$, the equation (5) becomes a non-linear one called Bürgers equation

$$\frac{\partial w(x,t)}{\partial t} + \frac{1}{2}\left(\frac{\partial w(x,t)}{\partial x}\right)^2 - \frac{h}{2}\frac{\partial^2 w(x,t)}{\partial x^2} = 0, \tag{6}$$

and then $w = \lambda_1 \otimes_h u_1 \oplus_h \lambda_2 \otimes_h u_2 = -h\ln(e^{-\frac{w_1+\lambda_1}{h}} + e^{-\frac{w_2+\lambda_2}{h}})$ is still a solution. One deduces immediately that Bürgers equation is linear in the doid defined by relations (4). At the limit $h \to 0$, equation (6) becomes a one-dimensional Hamilton-Jacobi one, and $w = \min(\lambda_1 + u_1, \lambda_2 + u_2)$.

If one changes the bijective mapping to

$$\begin{array}{rcl} \Phi_h \colon (\mathbb{R}, \oplus_h, \otimes_h) & \longrightarrow & (\mathbb{R}^+, +, \times) \\ x & \longmapsto & e^{\frac{x}{h}}, \end{array} \tag{7}$$

the deformation of $(\mathbb{R}, \oplus_h, \otimes_h)$ gives $\mathbb{R}_{\max,+}$ when $h \to 0^+$.

The starting point of idempotent analysis is based on the works of V. P. Maslov *et al*, and by many other authors. Maslov introduced $(\min, +)$-analysis in the Chapter (8) of his book about Linear Equations Theory in the semi-modulus and called it idempotent analysis.
Usual mathematical object such as integration, scalar product and Fourier-Legendre transform have their analogous in idempotent analysis.
One presents them below in the case of $(\min, +)$-analysis .

Without loss of generalization and for the sake of simplicity let's define $X = (\mathbb{R}, +, \times)$ and $Y = \mathbb{R}_{\min,+}$. One considers the function $f : X \longrightarrow Y$, and the Y-semi-module $B(X, Y)$ of all functions $X \longrightarrow Y$ that are bounded in the sense of the standard order on Y. The idempotent analog of a linear functional space is a set of Y-valued functions that is closed under addition of functions and multiplication of functions by elements of Y, or an Y-semi-module. From a heuristic point of view, a $\oplus$-Riemann sum of the form $\sum_i f(x_i) \cdot \Delta x_i$ corresponds to the expression

$$\bigoplus_i f(x_i) \otimes \Delta x_i = \min_i \{f(x_i) + \Delta x_i\}.$$

If $Y = \mathbb{R}_{\min,+}$ or $Y = \mathbb{R}_{\max,+}$, and $\forall \varphi \in B(X, S)$, the idempotent analog of integration is then respectively defined by

$$\int_X^{\oplus} f(x)\, dx \equiv \min_{x \in X} f(x), \text{ or } \int_X^{\oplus} f(x)\, dx \equiv \max_{x \in X} f(x). \tag{8}$$

One can replace the classical scalar product $\langle f, g\rangle = \int_{x\in X} f(x)\cdot g(x)\cdot dx$ with the $(\min, +)$ scalar product

$$\langle f, g\rangle_{(\min,+)} = \min_{x\in X}\{f(x) + g(x)\} \equiv \int_{x\in X}^{\oplus} dx \otimes f(x) \otimes g(x).$$

With this $(\min, +)$ scalar product, one obtains a distribution-like theory : the operator is linear and continuous in the dioid structure $\mathbb{R}_{\min,+} = (\mathbb{R}\cup\{+\infty\}, \min, +)$, non-linear and continuous in the classical structure $(\mathbb{R}, +, \times)$. The non-linear distribution $\delta_{(\min,+)}$ defined on $\mathbb{R}^n$ as

$$\delta_{(\min,+)}(\mathbf{x}) = \{0 \text{ if } \mathbf{x} = \mathbf{0}, +\infty \text{ else}\} \tag{9}$$

is similar in $(\min, +)$ analysis to the classical Dirac distribution. Then, one has

$$\begin{aligned}\langle \delta_{(\min,+)}, f\rangle_{(\min,+)} &= \min_{\mathbf{x}\in X}\{\delta_{(\min,+)}(\mathbf{x}) + f(\mathbf{x})\}\\ &= \min\{f(\mathbf{0}), +\infty\}\\ &= f(\mathbf{0}).\end{aligned} \tag{10}$$

- $(\min, +)$-analysis takes it roots from the shortest path research in a finite graph. First authors, M. Gondran *et al* have shown that the optimality equation to determine the shortest path is a linear equation with fixed-point solution in a particular algebraic structure : the dioid $\mathbb{R}_{\min} = (\mathbb{R} \cup \{+\infty\}, \min, +)$ which is an idempotent semi-ring different from real numbers field $(\mathbb{R}, +, \times)$.
- They have demonstrated that the classical resolution methods of linear algebra on the real numbers field can be re-written into this dioid $\mathbb{R}_{\min}$ yielding to computation algorithms in order to find the shortest path.
- In the same spirit, if one uses the dioid $\mathbb{R}_{\max,\min} = (\mathbb{R} \cup \{+\infty\}, \max, \min)$, it is possible to solve other problems such as to find maximal capacity path in a graph.

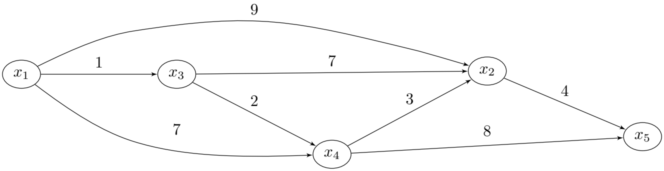
9
1
7
2
3
4
7
8
x_1
x_3
x_2
x_4
x_5

In Operation Research, graphs can be used to represent paths, flow circulations, and pre-order relations for instance. Almost all arcs or edges are valued, which means that they are endowed with a real number which might represent physical actions, distances, time intervals, or flow capacities, ... Several interesting problems occurring in this field consist to find an path in a graph with an optimal valuation (sum of valuations). Most algorithms designed to solve such kind of problems are based on the Bellman's Optimality Theorem, which is the keystone of Dynamic Programming Theory. It states that **for a given criterium in a graph, every part of an optimal path, is optimal for the same criterium**. Its proof is obvious with mean of contradiction reasoning : if the sub-path is not optimal, one can replace it with a better one, and then the path from which it is extracted is not optimal, which is contrary to the initial hypothesis.

Let's consider a directed graph $G = (X, U)$ with $n \in \mathbb{N}^*$, where $X = \{x_i, i \in [\![1, n]\!]\}$ and $U = \{(x_i, x_j) \in X^2, (i, j) \in [\![1, n]\!]^2\}$ are respectively the sets of numbered vertices and arcs. A real number l_{ij} is assigned to each arc $(x_i, x_j) \in U$, as the length between vertices x_i and x_j.

One defines i_0 as the origin vertex index, and we seek the shortest path length $l_{i_0 j}$ between the vertices x_{i_0} and the other vertices $\{x_j\}_{j \in [\![1,n]\!]}$ of the graph. One writes l_j instead of $l_{i_0 j}$. The Dynamic Programming Bellman's theorem yields for l_j to the following relations :

$$\left\{ \begin{array}{l} l_{i_0} = 0, \\ \forall j \neq i_0, l_j = \min\limits_{x_i \in \Gamma_j^{-1}} \{l_i + l_{ij}\}, \end{array} \right.$$

where $\Gamma_j^{-1} = \{x_i, (x_i, x_j) \in U\}$ is the set of direct predecessors of vertex x_j in G.

If one sets the length of missing arcs to $+\infty$, the previous equations can be rewritten as

$$\left\{ \begin{array}{l} l_{i_0} = 0, \\ \forall j \neq i_0, l_j = \min\limits_{i \in [\![1,n]\!]} \{ l_i + l_{ij} \}. \end{array} \right. \tag{11}$$

For the sake of simplicity, one can consider that lengths l_{ij} are all positive, which yields to $x_j \geq 0$, $\forall j \in [\![1, n]\!]$ and to

$$\begin{cases} l_{i_0} = \min\left(\min_{i \in [\![1,n]\!]} \{l_i + l_{ii_0}\}, 0\right), \\ \text{and } \forall j \neq i_0, l_j = \min\left(\min_{i \in [\![1,n]\!]} \{l_i + l_{ij}\}, +\infty\right). \end{cases} \quad (12)$$

Let us consider the dioid $(\bar{\mathbb{R}}^+, \oplus, \otimes) \equiv (\mathbb{R}^+ \cup \{+\infty\}, \min +)$, then, the equations (12) can be written in a linear way

$$\begin{cases} l_{i_0} = \sum_{i=1}^{n} l_i \otimes l_{ii_0} \oplus (0), \\ l_j = \sum_{i=1}^{n} l_i \otimes l_{ij} \oplus (+\infty) \text{ for any } j \neq i_0. \end{cases} \quad (13)$$

Let $\mathbf{A} = (l_{ij})^\intercal$ the transpose of the lengths matrix, with $(i,j) \in [\![1,n]\!]^2$, $\mathbf{B} = (B_i)$, and $\mathbf{L} = (l_i)$, $i \in [\![1,n]\!]$, with $B_{i_0} = 0 \equiv e_\otimes$ and $B_j = +\infty \equiv e_\oplus$, $\forall j \neq i_0$. Then the equation (13) can be written as a fixed point one

$$\mathbf{L} = \mathbf{A} \otimes \mathbf{L} \oplus \mathbf{B}. \quad (14)$$

Seeking for the shortest path from the vertex i_0 to others consists to solve the linear system (14) in the algebraic structure $\mathbb{R}_{\min,+}$.

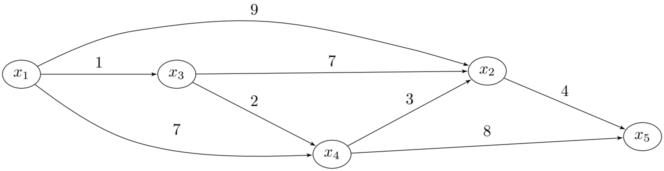

9
x_1
1
x_3
7
x_2
2
3
4
7
8
x_5
x_4

Considering the example with $i_0 = 1$, $j = 5$ and $l_{i_0} = l_1 = 0$. The previous equation (14) gives

$$\begin{pmatrix} l_1 \\ l_2 \\ l_3 \\ l_4 \\ l_5 \end{pmatrix} = \begin{pmatrix} 0 & +\infty & +\infty & +\infty & +\infty \\ 9 & 0 & +7 & 3 & +\infty \\ 1 & +\infty & 0 & +\infty & +\infty \\ 7 & +\infty & 2 & 0 & +\infty \\ +\infty & +4 & +\infty & +8 & 0 \end{pmatrix} \otimes \begin{pmatrix} 0 \\ l_2 \\ l_3 \\ l_4 \\ l_5 \end{pmatrix} \oplus \begin{pmatrix} 0 \\ +\infty \\ +\infty \\ +\infty \\ +\infty \end{pmatrix} \quad (15)$$

$$= \begin{pmatrix} 0 \\ \min\{9, l_2, 7 + l_3, 3 + l_4\} \\ \min\{1, l_3\} \\ \min\{7, 2 + l_3, l_4\} \\ \min\{4 + l_2, 8 + l_4, l_5\} \end{pmatrix} = \begin{pmatrix} 0 \\ 6 \\ 1 \\ 3 \\ 10 \end{pmatrix}, \quad (16)$$

which leads to the shortest path lengths starting from x_1 to the other vertices, such as $l_{15} \equiv l_5 = 10$ for instance.

In contrast to classical geometrical objects, the dimension of a fractal set is not an integer number. For a classical object, if covered with balls (or boxes) of size δ, the total number of balls required for the minimal covering increases as

$$N(\delta) \sim \delta^{-D}, \quad \text{for } \delta \to 0.$$

For regular geometrical objects the dimension D is always integer: $D = 1$ for line, $D = 2$ for surface, ... In general case D may, or may not be an integer. It is then convenient to characterize fractal sets by the power behavior of corresponding measures. Let us consider a set $\mathcal{A}$ and a function $M(d) = \sum_i \delta^d$, which is a measure defined on the coverage of the set $\mathcal{A}$ by δ-balls, $\delta \to 0$. If there exists such $d \in \mathbb{R}$, that the measure $M_d(\mathcal{A})$ has a discontinuity at $d = D_F$

$$\lim_{\delta \to 0} M_d(\mathcal{A}) = \sum_{\mathbf{x}_i \in \mathcal{A}} \delta_{\mathbf{x}_i}^d \sim N(\delta)\delta^d = \begin{cases} 0 & \text{for} \quad d > D_F \\ \infty & \text{for} \quad d < D_F, \end{cases},$$

the set $\mathcal{A}$ is said to have Hausdorff (or fractal) dimension D_H.

Figure: The construction of the triadic Cantor set from the unit length rode.

The fractal dimension of the $\frac{1}{3}$-Cantor set is easily derived from its construction procedure. In the i-th generation, we have $N = 2^i$ equal parts of length $l = 3^{-i}$. Thus, one gets

$$N = 2^i = 2^{-\frac{\ln l}{\ln 3}} = l^{-\frac{\ln 2}{\ln 3}} \Rightarrow D_H = \frac{\ln 2}{\ln 3} \approx 0.6309 < 1.$$

- Let $\mathbf{x} \in \mathbb{R}^m$, $f \in L^{\infty}_{loc}(\mathbb{R}^m, \mathbb{R}^n)$. $f \in \mathcal{C}^{\alpha}(\mathbf{x})$ if and only if it exists a constant $C > 0$ and $\alpha \in [0, 1]$, such as for $\mathbf{y}$ sufficiently close to $\mathbf{x}$, $\|f(\mathbf{y}) - f(\mathbf{x})\| \leq C\|\mathbf{y} - \mathbf{x}\|^{\alpha}$.
- Hölder exponent h_f of a function f at point $\mathbf{x} \in \mathbb{R}^m$ is defined as $h_f(\mathbf{x}) = \sup\{\alpha \geq 0 \ : \ f \in \mathcal{C}^{\alpha}(\mathbf{x})\}$
- The iso-Hölder exponents of h-order singularities for a function f is defined as $S_f(h) = \{\mathbf{x} \ : \ h_f(\mathbf{x}) = h\}$.
- The multi-fracal (or singularities) spectrum D_f of a function f is defined as the real positive number $D_f(h) = \dim_{\mathrm{H}} S_f(h)$.
- If D_f is constant according to h, the signal will be called mono-fractal.

A simple example to figure out what multi-fractal sets are, is the heuristic approach of Frisch and Parisi in hydrodynamic turbulence. They postulated that for a particular h and for each point $\mathbf{x} \in S_f(h)$, the small fluctuations of the flow velocity field $\mathbf{v}$ between the two points $\mathbf{x}$ and $\mathbf{x}+\mathbf{l}$ behave like

$$\|\mathbf{v}(\mathbf{x}+\mathbf{l}) - \mathbf{v}(\mathbf{x})\| \sim \|\mathbf{l}\|^h$$

If $D_{\mathbf{v}}(h) > 0$, one can state and with geometrical arguments that

$$\|\Delta \mathbf{v}_l\|_{L^q}^q = \int_\Omega \|\mathbf{v}(\mathbf{x}+\mathbf{l}) - \mathbf{v}(\mathbf{x})\|^q d^3\mathbf{x} \tag{17}$$

$$\sim \int_\Omega \|\mathbf{l}\|^{qh - D_{\mathbf{v}}(h)+3} dh = \|\mathbf{l}\|^{\xi_{\mathbf{v}}(q)} \tag{18}$$

For $\|\mathbf{l}\| \to 0$, the main contribution to this integral is obtained for

$$\xi_{\mathbf{v}}(q) = \min_{h \in [0,1]} \{qh - D_{\mathbf{v}}(h) + 3\},$$

which shows that $\xi_{\mathbf{v}}$ is the Legendre transform of $D_{\mathbf{v}}$, and explains therefore its concavity. Its inverse Legendre transform has the same property of concavity since

$$D_{\mathbf{v}}(h) = \min_{q \in \mathbb{R}} \{qh - \xi_{\mathbf{v}}(q) + 3\}.$$

This heuristic approach can be generalized for functions $f : \mathbb{R}^m \to \mathbb{R}$:

$$\xi_{\mathbf{v}}(q) = \min_{h \in [0,1]} \{qh - D_{\mathbf{v}}(h) + m\} \text{ and } D_{\mathbf{v}}(h) = \min_{q \in \mathbb{R}} \{qh - \xi_{\mathbf{v}}(q) + m\}.$$

In **MFA** the properties of singular objects are described in terms of the weighted measure $M_d(q,\delta)$, more general than $M_d(\delta)$:

$$M_d(q,\delta) = \sum_{\mathbf{x}_i \in \mathcal{A}} \mu_i^q \delta^d = Z(q,\delta)\delta^d \propto \delta^{d-\xi(q)}.$$

The multi-fractal formalism associates the fractal dimension $D(h)$ to the fractal subset of a given singularity strength h of the considered set. By thermodynamic analogy it is possible to consider

$$Z(q,\delta) = \sum_i \mu_i^q \propto \delta^{-\xi(q)}$$

as a *partition function*, with q regarded as a counterpart of the inverse temperature.

The power behavior of the partition function in $\delta \to 0$ limit is expressed in terms of the mass exponent $\xi(q)$, an analog of free energy in thermodynamics. The scaling exponent $\xi(q)$ and the fractal dimension $D(h)$ are related then by means of the Legendre transform :

$$\xi(q) = \min_h [qh - D(h)], \quad D(h) = \min_q [qh - \xi(q)].$$

The partition function $Z(q,a)$ can be directly evaluated using the calculated set of linear wavelet coefficients $W_\psi(a,\mathbf{b})$:

$$Z(q,a_0) = \sum_{\text{over all maxima } (\mathbf{b},a\leq a_0)} |W_\psi(a,\mathbf{b})|^q$$

In this construction, to calculate the partition function for a given scale a_0 one has to sum up over all maxima lines $l : (\mathbf{b}, a \leq a_0)$ starting from $(\mathbf{b}, a_0)$ and going to smaller scales $a < a_0$. In practice, this often means that it is sufficient to take a section $W_\psi(a = a_0, \mathbf{b})$ and sum up over all maxima in $\mathbf{b}$. The wavelet coefficients in the partition function (2) are taken in L^1 norm $W_\psi(a,\mathbf{b})[f] = \int \frac{1}{a}\bar{\psi}\left(\frac{\mathbf{x}-\mathbf{b}}{a}\right) f(\mathbf{x})d\mathbf{x}$ and are based on usual linear wavelets basis set such as gaussian derivatives wavelets for instance. It is named Wavelet-Transform Modulus-Maxima method (WTMM).

In $(\min, +)$ analysis, a set of non-linear transforms has been introduced for lower semi-continuous functions, the so-called $(\min, +)$-wavelets transforms which are defined for a function $f : \mathbb{R}^n \to \overline{\mathbb{R}}$ and for all $a \in \mathbb{R}^+$ and $\mathbf{b} \in \mathbb{R}^n$ such as :

$$T_f^-(a, \mathbf{b}) = \inf_{\mathbf{x} \in \mathbb{R}^n} \left\{ f(\mathbf{x}) + \hat{h}\Big(\frac{\mathbf{x} - \mathbf{b}}{a}\Big) \right\},$$

where $\hat{h}$ is a basis analysing function (upper semi-continuous and inf-compact verifying $\hat{h}(0) =$, like the following functions :

$$\hat{h}_\alpha(\mathbf{x}) = \frac{1}{\alpha}|\mathbf{x}|^\alpha \;\text{ with }\; \alpha > 1 \;\text{ and }\; \hat{h}_\infty(\mathbf{x}) = \{0 \;\text{ if }\; |\mathbf{x}| < 1, +\infty \;\text{ else}\}.$$

Since $T_f^-(a,\mathbf{x}) \leq f(\mathbf{x})$ for all $a > 0$, $T_f^-(a,\mathbf{x})$ is a lower hull of $f(\mathbf{x})$. For any lower bounded and lower semi-continuous function, one has a reconstruction formula like in the linear wavelets theory [?] :

$$f(\mathbf{x}) = \sup_{a\in\mathbb{R}^+,\mathbf{b}\in\mathbb{R}^n} \left\{ T_f^-(a,\mathbf{b}) - \hat{h}\Big(\frac{\mathbf{x}-\mathbf{b}}{a}\Big) \right\},$$

which can be simplified within the $(\min, +)$ theory in

$$f(\mathbf{x}) = \sup_{a\in\mathbb{R}^+} T_f^-(a,\mathbf{x}).$$

The $(\min, +)$-wavelets analysis will be based on simultaneous analysis of lower hulls $T_f^-(a, \mathbf{b})$, and upper hulls of f represented by $T_f^+(a, \mathbf{b})$ defined by :

$$T_f^+(a, \mathbf{b}) = \sup_{\mathbf{x} \in \mathbb{R}^n} \left\{ f(\mathbf{x}) - \hat{h}\Big(\frac{\mathbf{x} - \mathbf{b}}{a}\Big) \right\}.$$

For the upper hulls $T_f^+(a, \mathbf{b})$, we have a reconstruction formula which is symmetric to lower hulls $T_f^-(a, \mathbf{b})$:

$$f(\mathbf{x}) = \inf_{a \in \mathbb{R}^+, \mathbf{b} \in \mathbb{R}^n} \left\{ T_f^+(a, \mathbf{b}) + \hat{h}\Big(\frac{\mathbf{x} - \mathbf{b}}{a}\Big) \right\},$$

which simplifies as well as :

$$f(\mathbf{x}) = \inf_{a \in \mathbb{R}^+} T_f^+(a, \mathbf{x}).$$

$(\min, +)$-**wavelets** is defined as the couple $\{T_f^-(a, \mathbf{x}), T_f^+(a, \mathbf{x})\}$.
$\forall a \in \mathbb{R}^+$, the **a-oscillation** of f is defined as :

$$\Delta T_f(a, \mathbf{x}) = T_f^+(a, \mathbf{x}) - T_f^-(a, \mathbf{x}).$$

$T_f^-(a, \mathbf{x})$ (respectively $T_f^+(a, \mathbf{x})$) are functions decreasing with scales (respectively increasing) and converging to $f_*(\mathbf{x})$ (respectively $f^*(\mathbf{x})$), the lower semi-continuous closure of f (respectively upper semi-continuous closure) when the scale tends to 0. The following theorem guarantees that the $(\min, +)$-wavelets decomposition is well-defined :

Theorem

For each analysing function $\hat{h}$, one has :

$$T_f^-(a, \mathbf{x}) \leq f_*(\mathbf{x}) \leq f(\mathbf{x}) \leq f^*(\mathbf{x}) \leq T_f^+(a, \mathbf{x}).$$

We remind another important result linking local oscillations to Hölder exponents which is stated in the following theorem :

Theorem

The function f is Hölderian at point $\mathbf{x}_0$, with exponent H, $0 < H \leq 1$, if and only if it exists a constant C such as for all a, one has one of the following conditions :

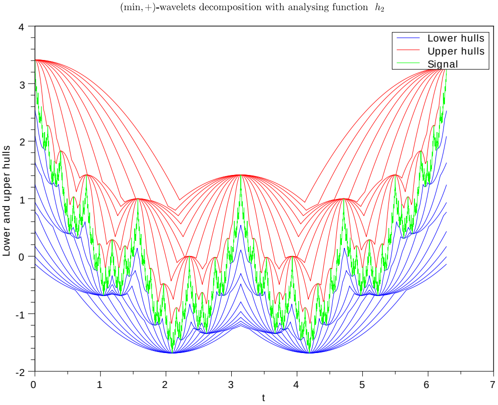

Figure: (min, +)-wavelets decomposition for the Weierstrass function $W(t) = \sum_{m \geq 0} 2^{-\frac{m}{2}} cos(2^m t)$ with the analysing function $\hat{h}_2$ for scales $k \cdot 10^{-1}$ with k from 1 to 10.

- Hölder exponent gives an incomplete information about the singularities' nature at a point. One needs then another analysing tool to quantify and classify them.
- The Hölder exponent calculations can be numerically unstable since it can be everywhere discontinuous. Thus, the computation of singularities spectrum is not possible directly from its definition, and one has to get it from other quantities.
- The $(\min, +)$-wavelets permits to generalise results established for mono-fractal functions to multi-fractal ones and to compute directly the scaling function ξ_f for f defined on a domain $\mathcal{T} \subset \mathbb{R}^m$:

$$\xi_f(p) = \lim_{s \to 0} \frac{\log \int_{\mathcal{T}} \left[\Delta T_f(s,t)\right]^p dt}{\log s}, \ \forall p \in \mathcal{P} \subset \mathbb{R}.$$

- The scaling function value for each $p \in \mathbb{R}$ can be viewed as the slope of linear part of the curve at small scales representing the logarithm of oscillations p-order moment $\int_{\mathcal{T}} \left[\Delta T_f(s,t)\right]^p dt$ according to the logarithm of scales s.

Thus, within the $(\min, +)$ -analysis framework and because of theorem (2), one can define α-**Legendre transforms** which yields to another definition of the scaling function and the singularities spectrum :

$$\xi_f(q) = \min_{h \in [0,1]} \left\{ q \frac{\alpha h}{\alpha - h} - D_f(h) + m \right\}$$

and

$$D_f(h) = \min_{q \in \mathbb{R}} \left\{ q \frac{\alpha h}{\alpha - h} - \xi_f(q) + m \right\}.$$

The basic flowchart is very simple

1. Compute $\Delta T_f(s,t)$ with $(\min,+)$-wavelets for scales $s \in \mathcal{S} \subset \mathbb{R}^{+*}$ and for $t \in \mathcal{T} \subset \mathbb{R}^m$.
2. Perform linear regression at small scales s ($s \to 0^+$) and numerical integration methods in order to obtain $\xi_{f,(\min,+)}(p)$.
3. Minimisation of equations in order to get singularities spectrum $D_{f,(\min,+)}$.

Riemann proposed in 1854 in his research thesis the definition of his famous integral. Cauchy had already established that the integral of a piecewise continuous function is well-defined. In order to show that his integral generalises the Cauchy's one, Riemann applied it to the so-called Riemann serie $R(x) = \sum_{m=1}^{\infty} \frac{nx-[nx]}{n^2}$, where $x \mapsto [x]$ is the ceiling function which gives the smallest integer not less than x. One can immediately prove that it is Riemann-integrable but has dense discontinuities set, which means that it is not Cauchy-integrable. It is one of the first example of multi-fractal function and it has been proved that its singularities spectrum is $D(h) = h$ for $h \in [0, 1]$, and scaling function is $\xi_R(p) = p \cdot \mathbb{I}_{[0,1]}(p) + \mathbb{I}_{[1,+\infty]}(p)$ for $p \geq 0$. The previous flowchart is applied to Riemann serie with 2^{10} points in Figure (3). Numerical results are exhibited on Figures (4) and (5) and proves that **MFA** of Riemann function with $(\min, +)$-wavelets decomposition is well-suited and efficient to find the right spectrum and scaling function for the Riemann serie.

The multi-fractal formalism was first successfully applied in physics to the description of cascade processes in hydrodynamic turbulence, Richardson's one for example. It is often named *binomial multiplicative process* or *Mandelbrot cascade* and is the simplest example of a multi-fractal set. This model describes a non-equal sharing of the energy flux from a large eddy of size l to 2^d small ones of size $l/2$, where d is space dimension. Let us give an example in one dimension by considering a population of arbitrary objects, initially distributed homogeneously on a unit interval $[0, 1]$ and a process, which redistributes the population with the probability p to the left half of the interval, and with probability $q = 1 - p$ to the right half. After the first iteration we will have the probability measure (p, q) for the whole interval, after the second iteration (p^2, pq, qp, q^2), ... An example of such cascade is shown on Figure with $p = 0.25$. It is easy to write the exact multi-fractal spectrum of this process as :

$$D(h) = -\{h \log_2 h + (1 - h) \log_2(1 - h)\}, \ \forall h \in]0, 1[,$$

which is obviously concave since it is the opposite of a convex combination.

One would like to illustrate efficiency of $(\min, +)$-wavelets approach compared to WTMM one. Thus, we applied to Riemann series and to the Mandelbrot cascade, the WTMM method with mean of gaussian wavelet of level 7, which is defined as the function

$$\forall t \in \mathbb{R},\ \ t \longmapsto \frac{d^7 \exp\left(-\frac{t^2}{2}\right)}{dt^7} = -t \exp\left(\frac{t^2}{2}\right) \cdot \left(t^6 - 21t^4 + 105t^2 - 105\right).$$

Figure: Representation of the Riemann serie $R(x) = \sum_{m=1}^{\infty} \frac{nx - [nx]}{n^2}$ with 2^{10} points.

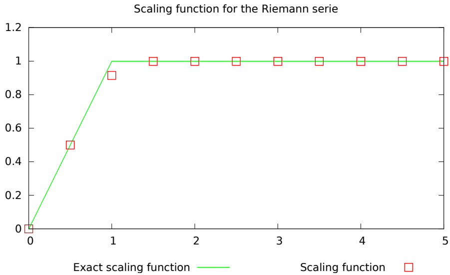

Figure: Exact and numerical scaling functions of the Riemann serie $R(x) = \sum_{m=1}^{\infty} \frac{nx-[nx]}{n^2}$ with $\hat{h}_\infty$ analysing function. Relative error in l^2-norm is about $\simeq 2.50\%$.

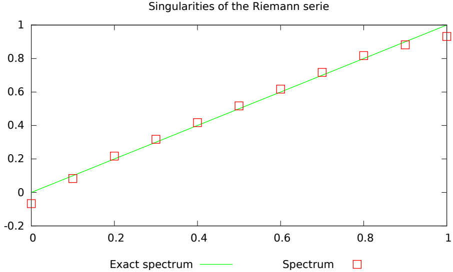

Figure: Exact and numerical singularities spectra of the Riemann serie $R(x) = \sum_{m=1}^{\infty} \frac{nx-[nx]}{n^2}$ with $\hat{h}_\infty$ analysing function. Relative error in l^2-norm is about $\simeq 4.92\%$.

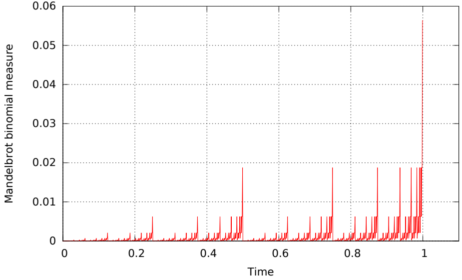

Figure: Mandelbrot cascade in one dimension for probability $p = 0.25$ and 10 levels.

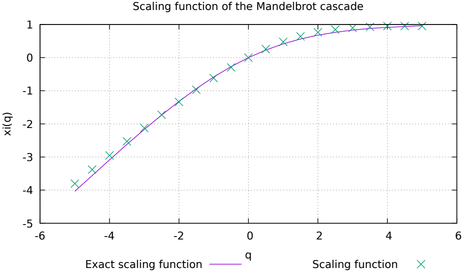

Figure: Mandelbrot cascade exact and numerical scaling function for probability $p = 0.25$ and 10 levels with $\hat{h}_\infty$ analysing function. Relative error in l^2-norm is about $\simeq 2.50\%$.

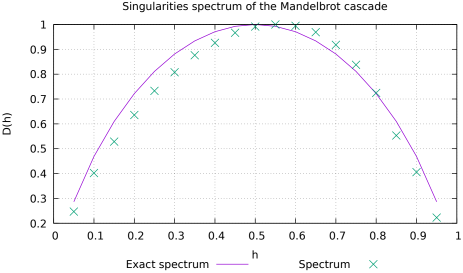

Figure: Mandelbrot cascade exact and numerical spectra for probability $p = 0.25$ and 10 levels with $\hat{h}_\infty$ analysing function. Relative error in l^2-norm is about $\simeq 5.62\%$.

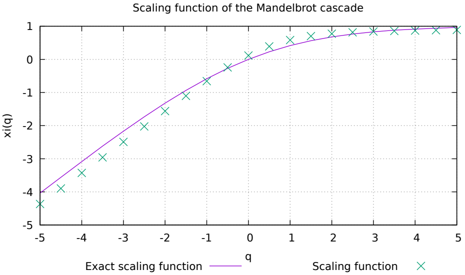

Figure: Mandelbrot cascade exact and numerical scaling function for probability $p = 0.25$ and 10 levels computed with WTMM method using continuous gaussian wavelet of level 7 as analysing function. Relative error in l^2-norm is about $\simeq 11.65\%$.

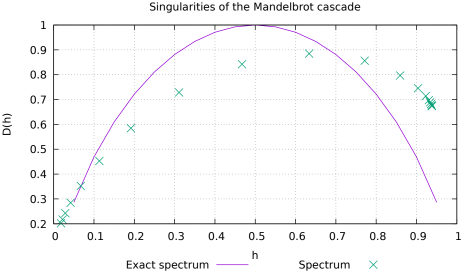

Figure: Mandelbrot cascade exact and numerical spectra for probability $p = 0.25$ and 10 levels computed with WTMM method using continuous gaussian wavelet of level 7 as analysing function. Relative error in l^2-norm is about $\simeq 37.68\%$.

- Image processing
- Control theory and optimisation
- Complex Variational Calculus
- Path integral formalism and Action-particle duality in quantum physics
- ...

MERCI BEAUCOUP POUR VOTRE ATTENTION !!